

# Certificate of Publication



**INTERNATIONAL JOURNAL OF RESEARCH AND ANALYTICAL REVIEWS (IJRRAR) | E-ISSN 2348-1269, P-ISSN 2349-5138**  
*An International Open Access Journal*

The Board of International Journal of Research and Analytical Reviews (IJRRAR)

Is hereby awarding this certificate to

**Shete S.B.**

In recognition of the publication of the paper entitled

**SYNTHESIS, CHARACTERIZATION OF RHA HIGH QUALITY NANO SIZED MESOPOROUS MATERIAL**

**SBA-16 USING ULTRASONICATION**

Published In IJRRAR ( www.ijrrar.org ) ISSN UGC Approved & 5.75 Impact Factor

Volume 6 Issue 1 February-2019

PAPER ID : IJRRAR19J1999

Registration ID : 196804

UGC and ISSN Approved - International Peer Reviewed Journal, Indexed Journal, Impact Factor: 5.75 Google Scholar

**INTERNATIONAL JOURNAL OF RESEARCH AND ANALYTICAL REVIEWS | IJRRAR**

*An International Open Access Journal* | Approved by ISSN and **DOAJ**

Website: [www.ijrrar.org](http://www.ijrrar.org) | Email: [editor@ijrrar.org](mailto:editor@ijrrar.org) | ESTD: 2014 (In Dist. Parbhani)



EDITOR IN CHIEF

*A.B. Joshi*

Co-ordinator  
IAC

Prof. Dr. B. D. Sawant Mahavidyalaya,  
Parbhani Dist. Parbhani - 431211 (M.S.)



# Synthesis, Characterization of RHA High Quality Nano Sized Mesoporous Material SBA-16 Using Ultrasonication

S.B.Shete

Department of Physics, S.G.B. College, Purna (Jn) – 431 511.

**Abstract:** Spherical particles of mesoporous silica SBA-16 with cubic  $Im\bar{3}m$  structure were synthesized at low pH using Pluronic F127 as template and TEOS as silica source. The diameter of the spherical particles can be controlled in the range of 0.5–8  $\mu\text{m}$  by varying synthesis temperature. Spherical particles of mesoporous silica SBA-16 with cubic  $Im\bar{3}m$  structure were synthesized at low pH using Pluronic F127 as template and RHA as silica source. The diameter of the spherical particles can be controlled in the range of 0.5 – 8  $\mu\text{m}$  by varying synthesis temperature at 45 °C. A sharp transition from large particle is observed. It is suggested that this morphology transition is due to a change in hydrolysis and condensation rate of the silica source and as a result the assembly of F127 micelles will differ. The SBA-16 samples were characterized using powder X-ray diffraction (XRD), scanning electron microscopy (SEM), transmission electron microscopy (TEM) and Nitrogen adsorption techniques.

**Keywords:** SBA-16; Spherical particles; Synthesis temperature; Morphology; F127

## INTRODUCTION:

The synthesis of mesoporous materials by a hydrothermal treatment [1, 2, 5]. The properties of these materials make them attractive for adsorption, catalysis, separation, chemical sensing, optical coating, drug delivery and electronic applications. For practical purposes, the overall morphology of a mesoporous material is a necessary requirement in combination with their internal structure. For instance, in application such as high performance liquid chromatography isometric particles are required [20] and spherical particles are preferably used in chromatography for column packing as irregular particles tend to break down [22]. In this body-centered-cubic structure each mesoporous is connected with its eight nearest neighbors to form a multidirectional system of mesoporous network [23]. Due to its large cage, high surface area and high thermal stability, this material appears to be one of the best candidates for catalytic support and packing materials for separation. Using F127 as a surfactant is the common way of synthesizing SBA-16 [16, 24]. However, there are also reports on alternative surfactants such as F108 [25], a blend of P123 and F127 [26], and other nonionic surfactants [27]. Several studies have been carried out to understand the formation mechanism of this material, for instance, in the framework of the colloidal phase separation mechanism (CPSM) Yu et al. [29] suggested that, the formation process of mesoporous materials involves three stages: (1) cooperative self-assembly of inorganic/organic composites, (2) Spherical particles of mesoporous silica SBA-16 structure were synthesized at low pH using Pluronic F127 as template and TEOS

silica source Similarly, M. Mesa et al. [30] followed the formation mechanism of SBA-16 from the earliest stage of the reaction until the formation of the particles by a dynamic light scattering technique, and suggested three steps for that: (1) silica coating of the surfactant micelles and crease of the zeta potential, (2) formation of micron-sized "liquid particles" by aggregation and fusion of the composite colloids (silica coated micelles), and (3) solidification of the "liquid particles" and transformation into the final particles of mesoporous silica. Synthesis conditions such as temperature, acidity, silica concentration, This material can be prepared using various synthetic procedures, which can drastically influence its final textural and morphological properties. If a ternary triblock copolymer/water/butanol system is used, and the synthesis is carried out at a lower acid concentration than in the traditional copolymer/water/HCl system, it is possible to enhance the structural order over the final product. The synthesis is driven by a self-assembly of the polymer in micelles [30], which minimizes the contact of its hydrophobic parts with the water solution and leads to the formation of the silica inorganic structure by hydrolysis of tetraethoxysilane (TEOS) at the later polymer

## Experimental details:

**Material synthesis:** The synthesis of silica SBA-16 was made following a ternary system based on a previously described method reported in literature. [17] A solution of 2.5 g of Pluronic F127 (Sigma Aldrich) in a mixture of 120 g of distilled water, 5 g of concentrated HCl (37%) and 7.5 g of butanol was first prepared. After one hour stirring at 45 °C, 12 g of RHA were added and the mixture stirred for further 24 h. The ultrasonic treatment is given at 45 min. The step was followed by a hydrothermal treatment of 24 h at 100°C in Teflon coated stainless steel autoclave. Drying of the as synthesized sample was performed at room temperature overnight part of the dry sample was calcined under air flow by increasing the temperature 1.5°C per minute up to 550°C and maintaining it at this temperature for 6 h sample hereafter named calc-SBA-16 by Fabio et al., [1]

Coordinator  
IQAC

Shri Guru Buddhiswami Mahavidyalaya  
431511 (M.S.)



PRINCIPAL

Shri Guru Buddhiswami Mahavidyalaya  
Purna, Jharkhand

# Synthesis, Characterization of RHA High Quality Nano Sized Mesoporous Material SBA-16 Using Ultrasonication

S.B.Shete

Department of Physics, S.G.B. College, Purna (Jn) – 431 511.

**Abstract:** Spherical particles of mesoporous silica SBA-16 with cubic  $Im\bar{3}m$  structure were synthesized at low pH using Pluronic F127 as template and TEOS as silica source. The diameter of the spherical particles can be controlled in the range of 0.5–8  $\mu\text{m}$  by varying synthesis temperature. Spherical particles of mesoporous silica SBA-16 with cubic  $Im\bar{3}m$  structure were synthesized at low pH using Pluronic F127 as template and RHA as silica source. The diameter of the spherical particles can be controlled in the range of 0.5 – 8  $\mu\text{m}$  by varying synthesis temperature at 45 °C. A sharp transition from large particle is observed. It is suggested that this morphology transition is due to a change in hydrolysis and condensation rate of the silica source and as a result the assembly of F127 micelles will differ. The SBA-16 samples were characterized using powder X-ray diffraction (XRD), scanning electron microscopy (SEM), transmission electron microscopy (TEM) and Nitrogen adsorption techniques.

**Keywords:** SBA-16; Spherical particles; Synthesis temperature; Morphology; F127

## INTRODUCTION:

The synthesis of mesoporous materials by a hydrothermal treatment [1, 2, 5]. The properties of these materials make them attractive for adsorption, catalysis, separation, chemical sensing, optical coating, drug delivery and electronic applications. For practical purposes, the overall morphology of a mesoporous material is a necessary requirement in combination with their internal structure. For instance, in application such as high performance liquid chromatography isometric particles are required [20] and spherical particles are preferably used in chromatography for column packing as irregular particles tend to break down [22]. In this body-centered-cubic structure each mesoporous is connected with its eight nearest neighbors to form a multidirectional system of mesoporous network [23]. Due to its large cage, high surface area and high thermal stability, this material appears to be one of the best candidates for catalytic support and packing materials for separation. Using F127 as a surfactant is the common way of synthesizing SBA-16 [16, 24]. However, there are also reports on alternative surfactants such as F108 [25], a blend of P123 and F127 [26], and other nonionic surfactants [27]. Several studies have been carried out to understand the formation mechanism of this material, for instance, in the framework of the colloidal phase separation mechanism (CPSM) Yu et al. [29] suggested that, the formation process of mesoporous materials involves three stages: (1) cooperative self-assembly of inorganic/organic composites, (2) Spherical particles of mesoporous silica SBA-16 structure were synthesized at low pH using Pluronic F127 as template and TEOS

silica source Similarly, M. Mesa et al. [30] followed the formation mechanism of SBA-16 from the earliest stage of the reaction until the formation of the particles by a dynamic light scattering technique, and suggested three steps for that: (1) silica coating of the surfactant micelles and crease of the zeta potential, (2) formation of micron-sized "liquid particles" by aggregation and fusion of the composite colloids (silica coated micelles), and (3) solidification of the "liquid particles" and transformation into the final particles of mesoporous silica. Synthesis conditions such as temperature, acidity, silica concentration, . This material can be prepared using various synthetic procedures, which can drastically influence its final textural and morphological properties. If a ternary triblock copolymer/water/butanol system is used, and the synthesis is carried out at a lower acid concentration than in the traditional copolymer/water/HCl system, it is possible to enhance the structural order over the final product. The synthesis is driven by a self-assembly of the polymer in micelles [30], which minimizes the contact of its hydrophobic parts with the water solution and leads to the formation of the silica inorganic structure by hydrolysis of tetraethoxysilane (TEOS) at the later polymer

## Experimental details:

**Material synthesis:** The synthesis of silica SBA-16 was made following a ternary system based on a previously described method reported in literature. [17] A solution of 2.5 g of Pluronic F127 (Sigma Aldrich) in a mixture of 120 g of distilled water, 5 g of concentrated HCl (37%) and 7.5 g of butanol was first prepared. After one hour stirring at 45 °C, 12 g of RHA were added and the mixture stirred for further 24 h. The ultrasonic treatment is given at 45 min. The step was followed by a hydrothermal treatment of 24 h at 100°C in Teflon coated stainless steel autoclave. Drying of the as synthesized sample was performed at room temperature overnight part of the dry sample was calcined under air flow by increasing the temperature 1.5°C per minute up to 550°C and maintaining it at this temperature for 6 h sample hereafter named calc-SBA-16 by Fabio et al., [1]

Coordinator  
IQAC

Shri Guru Buddhiswami Mahavidyalaya  
431511 (M.S.)



PRINCIPAL

Shri Guru Buddhiswami Mahavidyalaya

**Experimental:**

**XRD-studies:**

The X-ray pattern of the As-Synthesized and synthesized mesoporous silica material is a highly periodic silica phases which is normally reflected by the distinct XRD signatures at low  $2\theta$  angles from  $1^\circ$  to  $10^\circ$  as shown in Fig1 Sharp signal in XRD spectra indicates the presence of long range order of uniform hexagonal phase in the mesoporous materials. The well defined reflections from [110] plane are a prime characteristics of the hexagonal lattice symmetry of the SBA-16 structure with  $d_{110}$  value=26.3,  $2\theta = 1.121$ , Intensity: 40000 cps  $I/I_0=100$  Unit cell parameter  $a_0= 37.8\text{\AA}$

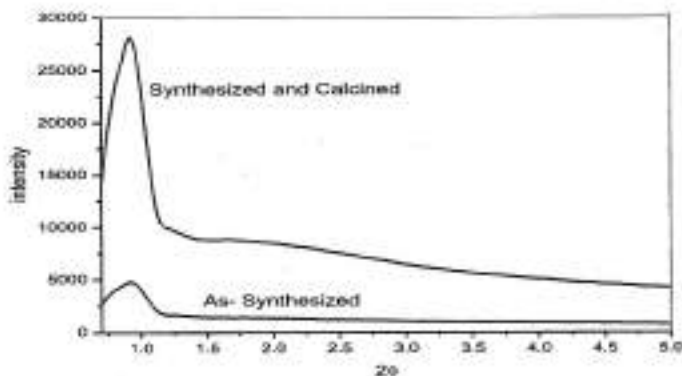


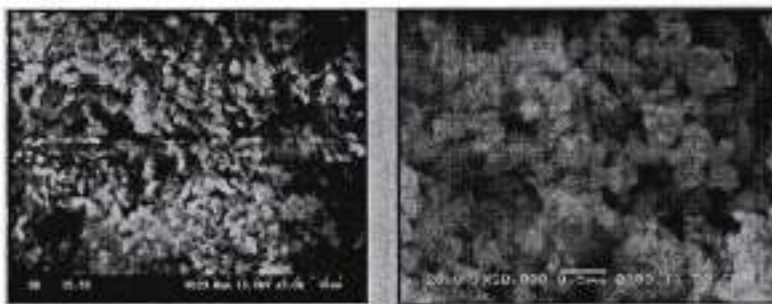
**Fig.1 XRD pattern of optimized RHA-SBA-16As-Synthesized and Synthesized Material**

However, it is evident that RHA-SBA-16 samples synthesized using surfactant Pluronic F-127 in a range from 1g to 4g showed the corresponding peaks for the planes (110), (120) and (200) located at 1.5, 3.2 and 3.9 $^\circ$  of  $2\theta$  respectively (Fig.1 Synthesized RHA-SBA-16).

Both, decreasing or increasing of surfactant Pluronic F-127 out of this range resulted in a decrease of the pore mesostructured ordering due to the disturbing of the assembly on RHA-SBA-16 structure during process of synthesis. On the other hand, as the amount of surfactant Pluronic F-127 used was 2.5g all the three peaks are shifted to lower  $2\theta$  values. This behaviour could be attributed to a thicker pore wall. In the case RHA-SBA-16 sample synthesized with surfactant Pluronic F-127 used less than 1.0g, it did not show the signals for the planes (110) and (200). This Pluronic F-127 behaviour is due to the increase in the surfactant concentration causing prohibition of unit cell growth and decrease in polymerization of silica resulting in poor hexagonal ordered RHA-SBA-16silica.

**SEM and TEM-analysis:**

Fig.2 (A, B) (As-Synthesized and Synthesized RHA-SBA-16) presents typical micro graphs of the as-synthesized and calcined RHA-SBA-16 samples. Formation of the RHA-SBA-16 phase at hydrothermal conditions under autogenic pressure is seen to result, in shorter time, in a solid consisting of small agglomerates Fig.2 (A) (Synthesized RHA-SBA-16). The RHA-SBA-16 samples exhibit agglomerates with sizes between 2.7 and 19.2 $\text{\AA}$ . Synthesized RHA-SBA-16 Sample exhibited uniform spherical shaped particles, with very small variations in the morphology and size might be associated with the differences in the synthesis gel conditions and hence in nucleation and crystallization.



(A)

(B)

**Fig.2 (A, B)SEM images of As-Synthesized and Synthesized Material(RHA-SBA-16)**

**TEM-analysis:**

Fig.2 (C) represents the TEM images of RHA-SBA-16. TEM images of the parent samples provided strong evidence of the formation of mesoporous structure of the supports. The characteristic hexagonal silicate structures shown on TEM, supports the observation made by low angle XRD.

Co-ordinator  
 Principal  
 Shri Guru Buddhiswami Mahavidyalaya  
 Std. 1983

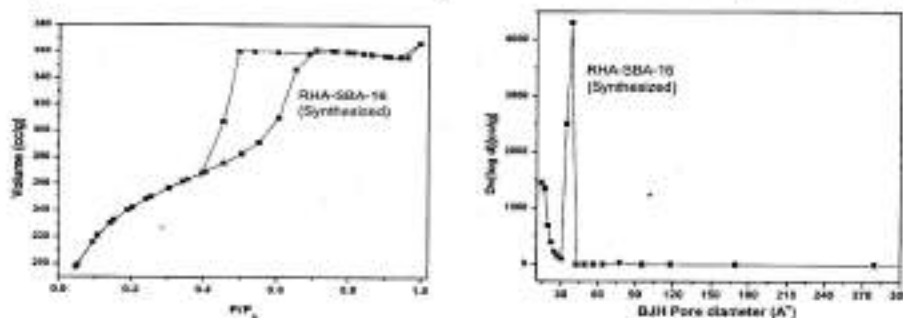


(C) TEM images of As-Synthesized and Synthesized Material (RHA-SBA-16)

**Sorption studies**

The adsorption/desorption isotherms of N<sub>2</sub> shown in Fig. 2 and the values of specific BET surface area, mean diameter of the mesopores, total volume of pores and wall thickness obtained for calcined RHA-SBA-16 are presented in Table 1 are well in agreement with XRD analysis. Curves in Fig.2 and data from Table 1 shows an increase in the adsorption capacity of N<sub>2</sub> with time for the RHA-SBA-16 samples synthesized, indicating an improvement in the order of the mesoporous phase, already observed by the increase in the XRD peak intensity (Fig. 2) According to IUPAC classification, the isotherm of RHA-SBA-16 is of type IV which is the characteristics of mesoporous material. For this sample, there is a continuous, slow adsorption of nitrogen after the point of inflection indicating a broad pore size distribution. The hysteresis loop is found over a wide range of relative pressures, p/p<sub>0</sub> (0.28-1.00). The shape of the hysteresis loop confirms the formation of a hexagonal phase. Thus, the XRD results are confirmed by N<sub>2</sub>-adsorption-desorption data, which are similar to those reported for SBA-16.

We noted that the surface areas of calcined RHA-SBA-16 samples are comparatively more than as synthesized RHA-SBA-16. The more surface area (779.70m<sup>2</sup>/g) is an indication of well dispersion of active sites. The standards for the optimization of the sample are summarized in Table 1 along with calculated unit cell parameter, average pore diameter and



wall thickness etc.

Fig.3. : N<sub>2</sub> adsorption-desorption isotherms of optimized RHA-SBA-16

Table 1 : Data obtained from XRD and N<sub>2</sub>-sorption studies for optimized sample

Sample conditions	preparation	d <sub>110</sub>	Unit cell parameter	S.A. (m <sup>2</sup> /g)	Average pore diameter (Å)	Pore volume (ml/g)	Average wall thickness (Å)
i. Synthesis temperature : 80 <sup>o</sup> c ii. Calcination Temperature : 550 <sup>o</sup> c iii. pH of gel in synthesis of material : 6.9 iv. calcination duration : 4.5h		26.93	38.78	779.70	29.16	0.568	9.62

**Effect of Ultrasonic Irradiation Power**

The ultrasonic irradiation synthesis of mesoporous molecular sieve RHA-SBA-16 was investigated by using polymeric Pluronic F-127 and organic silica source such as RHA in neutral condition. To study the effect of irradiation power, initially the gel was prepared as described earlier in the section with molar composition as follows



PRINCIPAL  
Shri Guru Buddhiswami Mahavidyalaya  
Purna  
(Dr.) Datt Parbhani

**MOLAR COMPOSITION :**

0.91SiO<sub>2</sub>:0.0035 (F-127) : 2.08BuOH: 0.91HCl : 117H<sub>2</sub>O.

The prepared gel was treated with different ultrasonic irradiation power 50W, 100W, 50W, 200W before optical conditions of hydrothermal method. The pH of the gel in each attempt of hydrothermal was maintained at 6.9 and hydrothermal temperature maintained at 80°C for 18h.

**XRD-STUDIES:**

Figure 4 shows the powder XRD pattern of four calcined samples which exhibit a typical peak pattern with a very strong (110) diffraction peak and other (120) and (200) diffraction weak peaks. Although sample RHA-SBA-16 (50 W, 100 W) shows strong (110) diffraction peak and two (120), (200) diffraction weak peaks, but the higher angle peaks are not resolved by broadening may be due to loss of order. Also the (110) reflection was of weak intensity with inferior  $d_{110}$  value indicating the existence of a predominantly amorphous content of silica in the products. As the power of ultrasonic radiation increased from 150W to 200W, the diffraction peaks were significantly strong. The XRD pattern of sample RHA-SBA-16 (200 W) exhibits typical three peaks along with a small fourth peak with notable intensity. Thus, it indicates that high quality of RHA-SBA-16 was synthesized. The data collected from the XRD analysis was tabulated in Table 2

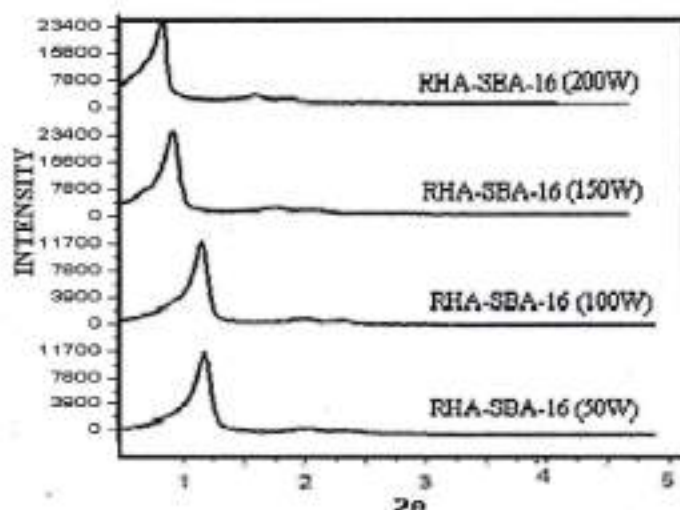


Fig. 4: XRD-pattern of RHA-SBA-16 synthesized at various ultrasonic power irradiation

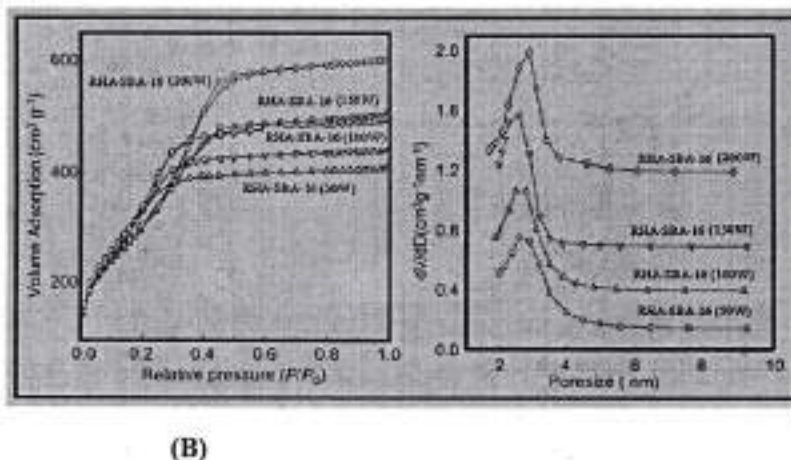
**SORPTION STUDIES:**

Fig. 5 : (A) Nitrogen adsorption and desorption isotherm of RHA-SBA-16 samples synthesized at various ultrasonic power irradiation and (B) Pore size distribution

The nitrogen adsorption-desorption isotherms for the calcined samples are shown in Figure 5 (A) and corresponding pore distribution in Figure 5(B). The N<sub>2</sub> adsorption isotherm of samples RHA-SBA-16 (50 W, 100 W) exhibits a broad steep corner according to N<sub>2</sub> condensation in primary mesopores, indicating a rather low degree of structural order. The 200W sample shows a typical hysteresis loop for relative pressures between 0.38 and 0.68 indicating the presence of a

smaller pore size value. As the power of ultrasonic irradiation increases, it was found that the steps width corresponding to  $N_2$  condensation in primary mesopores decrease gradually and hysteresis loop become smaller which indicates that for the higher ultrasonic power there was increase in the structure consistency demonstrated by the sharp PSD curve.

**Table 2 : Effect of ultrasound irradiation power on the structural and textural properties of RHA-SBA-16 at synthesis temperature 80°C**

Sample designation	$d_{110}$ (Å)	Unit cell parameter $a_0$ (Å)	Specific Surface area ( $m^2g^{-1}$ )	Pore Size (Å)	Pore volume (cc/g)	Wall thickness (Å)	% Crystallinity
RHA-SBA-16 (50W)	23.96	34.50	803.11	25.93	0.502	8.57	47
RHA-SBA-16 (100W)	24.16	34.79	816.59	26.10	0.537	8.69	71
RHA-SBA-16 (150W)	25.02	36.03	878.25	26.49	0.544	9.53	89
RHA-SBA-16 (200W)	25.30	36.42	954.22	26.53	0.568	9.89	100

From Table 2, it is comprehensible that as the power of ultrasonic irradiation increases from 50 W to 200 W there was shift of the most intense peak to higher  $d_{110}$  spacing value as well as small variation in the pore diameter which is due to increase in the wall thickness of the pores of RHA-SBA-16 molecular sieves, it results into higher specific surface area and pore volume, thermal stability of the product which may be due to special acoustic cavitation phenomenon of ultrasound radiations i.e. the formation, growth, and implosive collapse of bubbles in a liquid medium. During the formation of the framework of RHA-SBA-16, the ultrasound helps to disperse the small silica oligomers more homogeneously in the mixture. The cavitation phenomenon formed due to passage of acoustic vibrations accompanied by a few extreme effects, such as a local increase of temperature to about 5000 K and a local high pressure near 100 MPa which were called as hot spots. These hot spots within the surfactant-silicate interface accelerate the silica polymerization, which was slow and rate-limiting under normal conditions. The rate of formation of hot spots increases with increase in the power of ultrasound irradiation. This twofold function of ultrasound radiation results in the particles of sonochemical product being bigger and more aggregated than those prepared conventionally. Thus, the fabrication of the mesostructure can be achieved more efficiently. It was also worth noting that ultrasound radiation did not destroy the micellar structure. The Fig.6 shows the effect of ultrasonic irradiation power given to reaction gel, when treated with optimization condition of hydrothermal synthesis on crystallization of RHA-SBA-16. It was observed with increase in irradiation power and reaches to maximum value (consider as 100%) as shown in figure.

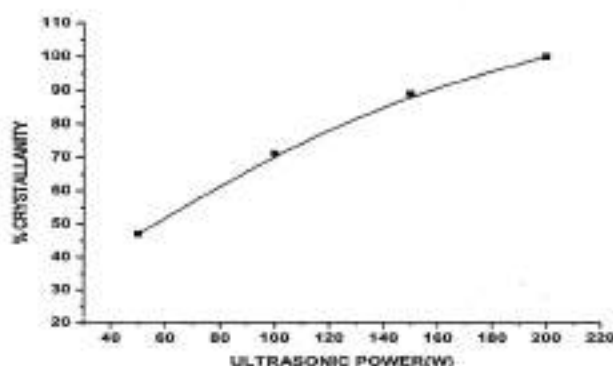


**Fig. 6 : Effect of Ultrasonic irradiation power on crystallization**

#### SEM AND TEM ANALYSIS:

Fig.2.31 (A) presents typical micrographs of the calcined RHA-SBA-16 (150 W, 200 W) samples. Formation of the RHA-SBA-16 phase at hydrothermal cum ultrasonic conditions under autogenic pressure is seen to result, in shorter time, in a solid consisting of small agglomerates Fig. 7 (A-RHA-SBA-16 (150 W, 200 W)).

The RHA-SBA-16 samples exhibit agglomerates with sizes between 24 and 270 nm. Sample RHA-SBA-16(150 W) exhibited uniform spherical shaped particles, with very small variations in the morphology and size might be associated with the presence of minor impurities in the extracted silica from rice husk and hence in nucleation and crystallization.

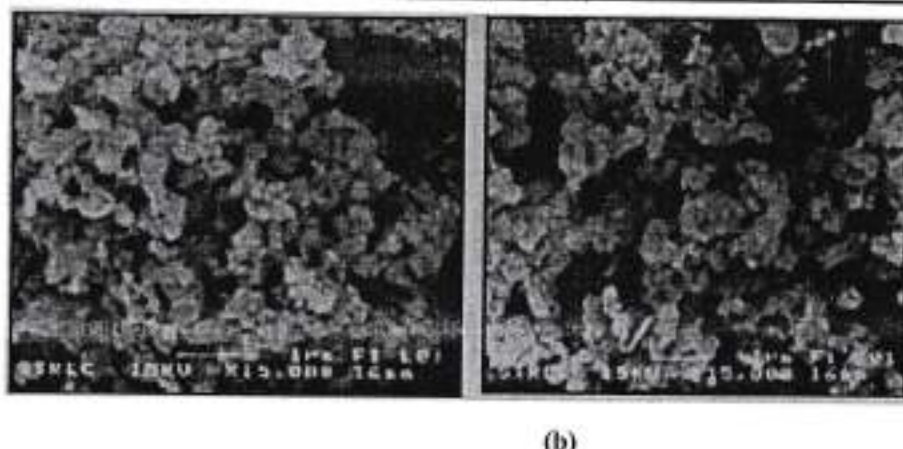


Fig. 7 : (A) SEM images of As-Synthesized and Synthesized Material (RHA-SBA-16)

#### TEM-ANALYSIS:

Fig. 8 (shows spectacular the TEM image of calcined RHA-SBA-16. The mesopores are arranged in a honeycomb like structure, separated by thick, amorphous silica pore walls. From the TEM image, it was apparent that RHA-SBA-16 has a very large void fraction, due to the presence of mesopores.



Fig. 8: TEM images of Synthesized Material (RHA-SBA-16(200W))

#### FTIR-STUDIES:

The synthesized samples were further characterized by Fourier transform spectroscopy. The FTIR spectra of RHA-SBA-16 synthesized at various ultrasonic power irradiations illustrated in Fig. 9. The broad band around  $3500\text{ cm}^{-1}$  is due to surface silanol and adsorbed water molecules which indicating the silica framework is hydrophilic. The two peaks at  $2922.9\text{ cm}^{-1}$  and  $2852.5\text{ cm}^{-1}$  indicates the presence of organic template in the framework. RHA-SBA-16 tends to adsorb water vapours in air since the surface of silica framework is water liking; the stretching mode of  $\text{H}_2\text{O}$  is detected at  $1634\text{ cm}^{-1}$ . Bands observed at  $1234\text{ cm}^{-1}$  and  $1071\text{ cm}^{-1}$  are characteristics peaks of asymmetric Si-O-Si stretching. Another characteristics peak is the symmetric Si-O-Si stretching recorded at  $786\text{ cm}^{-1}$ . However, the peak at  $2319\text{ cm}^{-1}$  is prominently found to be changed due to the effect of ultrasonic power on the synthesis of RHA-SBA-16. The effect observed for RHA-SBA-16 is manifested by the XRD analysis and sorption studies of the samples.

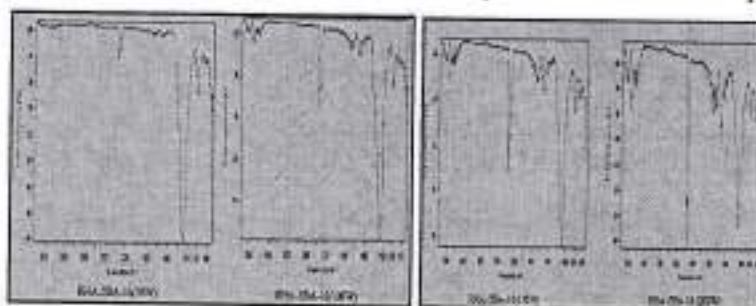


Fig. 9 : FTIR spectra of RHA-SBA-16 samples synthesised at various ultrasonic irradiation power

#### Effect of Ultrasonic Irradiation time applied to reaction gel:

The initial gel was prepared as described earlier. The obtained gel (pH = 6.9) was stirred for 30 min at synthesis temperature followed by ultrasound irradiation by Sonicator LNP-250, by keeping the power constant i.e. 200W which was optimized in preceding section. Four samples were synthesized under different ultrasonic irradiation time of 5, 10, 15 and 20 min. While the ultrasonic power kept constant and the gel obtained for different time interval was subjected to the hydrothermal treatment obtain the final sample. The hydrothermal synthesis parameters are the same as maintained in the earlier section and were designated as RHA-SBA-16/Syn. Time. 5, 10, 15 and 20 min. The effect of ultrasonic irradiation time on the synthesis of RHA-SBA-16 is studied by FTIR, XRD, SEM, TEM, and sorption studies.

procedure followed is same as described earlier. The materials synthesized have been evaluated by x-ray diffraction and nitrogen sorption studies.

### XRD-STUDIES:

Figure 10 shows the XRD pattern of all the four samples synthesized for different ultrasound irradiation time interval and the corresponding data tabulated in Table 3. As shown in the Figure 10, the XRD pattern of sample RHA-SBA-16(5min) which was synthesized at irradiation time 5 min, the only reflection at (110) plane is more intense, it suggests that the material does not possess the well-defined hexagonal arrays even after the calcination. As the irradiation time is increased from 5 min to 15 min, the intensity of characteristic peak increased and the reflection (110) was shifted to lower  $2\theta$  value consequently shifting of  $d_{110}$  to higher value. The XRD pattern of calcined RHA-SBA-16 (20min) exhibit a typical four peak pattern with a very strong (110) reflection at low angle and other weaker reflections. The presence of (210) reflection suggest the excellent quality of synthesized RHA-SBA-16. If the irradiation time increased further there is gradual decrease in the value of  $d_{110}$  spacing. Surprisingly dramatic decrease in the  $d_{110}$  spacing decrease was observed for the irradiation time 30 min. This is may be due to the long-time ultrasonic irradiation minimizes the micellar size so that more but smaller micelles exist in the solution, resulting in an arrangement of silicate around the micelles and forming the mesophase structure with smaller unit cell size.

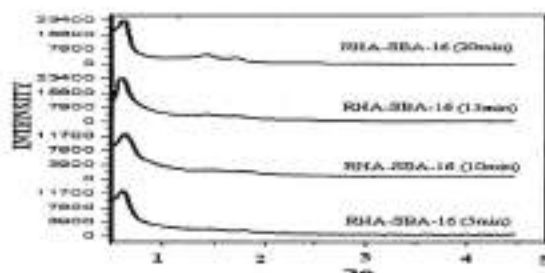


Fig. 10 : XRD pattern of calcined samples synthesised at various ultrasound irradiation time

Table 3: Effect of ultrasound irradiation time on the reaction gel

Sample designation	$d_{110}$ (Å)	Unit cell parameter $a_0$ (Å)	Specific Surface area ( $m^2g^{-1}$ )	Pore Size (Å)	Pore volume ( $cc/g$ )	Wall thickness (Å)	% crystallinity
RHA-SBA-16(5min)	24.58	35.39	879.37	26.25	0.498	9.15	51
RHA-SBA-16(10min)	25.00	36.00	893.22	26.74	0.513	9.26	73
RHA-SBA-16(15min)	25.19	36.27	981.00	26.90	0.533	9.37	91
RHA-SBA-16(20min)	25.30	36.42	954.22	26.53	0.568	9.89	100

From Table 3, due to cavitation phenomenon of acoustic vibration of ultrasound waves in the gel, the specific surface area as well as pore wall thickness increases gradually as the irradiation time increases from 5 min to 20 min. Ultrasonic irradiation for longer time minimizes the micellar size so that more number of micelles exists in the solution but is of smaller size. Table 3 also summarizes the values of % crystallinity derived from X-ray diffraction pattern for various synthesized RHA-SBA-16 samples which were further plotted as a function of ultrasonic power as shown in Figure 2.34. The curve indicates the percent conversion from amorphous to 100 % crystalline product. Up to irradiation time 10 min the rate of conversion of amorphous to crystallized phase of RHA-SBA-16 was slow. Beyond that the rate increases rapidly due to formation of more hot spots within the surfactant-silicate interface which accelerate the silica polymerization in the synthesis gel. The degree of crystallization decreases as the process approaches to the completion indicated by constancy in percent crystallization. The apparent activation energy for conversion was estimated from the slope of linear plot of  $\ln K$  vs.  $(1/T)$  by applying the Arrhenius equation  $d \ln K / d(1/T) = E_a / RT$ , where  $K$  is the rate of conversion,  $E_a$  is the energy of crystallization/ conversion,  $R$  is the universal gas constant. By the application of Arrhenius equation to the kinetics of crystallization of RHA-SBA-16, an apparent activation energy of conversion of aluminosilicate gel to 100% crystalline phase was estimated to be  $124.11 kJ \text{ mole}^{-1}$  in the present crystallization system.

SEM and TEM analysis of RHA-SBA-16 (20min) exhibits distinctive micrographs of the calcined RHA-SBA-16 samples. Formation of the RHA-SBA-16 (20min) exhibits distinctive micrographs of the calcined RHA-SBA-16 samples. Formation of the RHA-SBA-16 (20min) exhibits distinctive micrographs of the calcined RHA-SBA-16 samples.

solid consisting of small agglomerates with sizes between 2.04 and 27.60 Å. Sample RHA-SBA-16 (20min) exhibited uniform spherical shaped particles, with very small variations in the morphology and size might be associated with the retention of some impurities in the extracted silica from rice husk and hence in nucleation and crystallization.

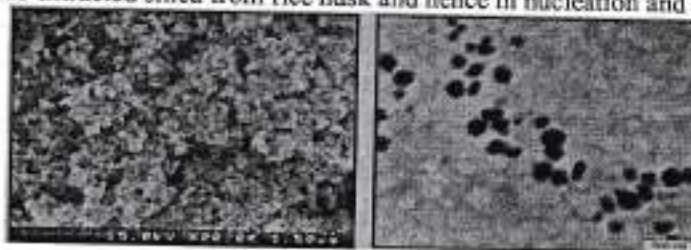


Fig.11 (A, B) SEM and TEM images of Synthesized Material RHA-SBA-16 (20min)

#### TEM-ANALYSIS:

Fig. 11 (B) shows brilliant TEM image of calcined RHA-SBA-16. The mesopores are arranged in a honeycomb like structure, separated by thick, amorphous silica pore walls. From the TEM image, it was apparent that RHA-SBA-16 has a very large void fraction, due to the presence of mesopores.

#### Conclusions:

Based upon the experimental study it was concluded that pure and ordered SBA16 material could be successfully synthesized by triblock copolymer F127 during 18 hrs of reaction. The parametric variations such as change of calcination temperature, the change of calcination time duration and the change of initial pH value of gel suggested that from RHA the well ordered mesoporous material SBA16 can be synthesized at 5500C for 4 hrs. keeping pH of gel 6.91. The maximum calculated surface area amounts to 779.7 m<sup>2</sup>/g for the SBA16 materials keeping pH of gel 6.91, calcination time about 4 h. at 5500C.

#### References:

1. Fabio Carniato, Geo Paul, Chiara Bisio Stefano Caldarelli and Leonardo Marchese 2012, 2, 1153–1160
2. F. Hoffmann, M. Cornelius, J. Morell and M. Froba, *Angew. Chem.Int. Ed.*, 2006, 45, 3216.
3. Q. Yang, J. Liu, L. Zhang and C. Li, *J. Mater. Chem.*, 2009, 19, 1945
4. H. Xiong, Y. Zhang, S. Wang, K. Liew and J. Li, *J. Phys. Chem. C*, 2008, 112, 9706
5. Zhou, J. M. Thomas, D. S. Shephard, B. F. G. Johnson, D. Ozkaya, T. Maschmeyer, R.G. Bell and Q. Ge, *Science*, 1998, 280, 705.
6. B. J. Scott, G. Wirnsberger and G. D. Stucky, *Chem. Mater.*, 2001, 13, 3140.
7. X. Gao and S. Nie, *J. Phys. Chem. B*, 2003, 107, 11575.
8. B. Lei, B. Li, H. Zhang, L. Zhang and W. Li, *J. Phys. Chem. C*, 2007, 111, 11291.
9. J. Feng, H. J. Zhang, C. Y. Peng, J. B. Yu, R. P. Deng, L. N. Sun and X. M. Guo, *Microporous Mesoporous Mater.*, 2008, 113, 402.
10. S. Wang, *Microporous Mesoporous Mater.*, 2009, 117, 1.
11. M. Vallet-Regi, F. Balas and D. Arcos, *Angew. Chem., Int. Ed.*, 2007, 46, 7548.
12. J. Kim, Y. Piao and T. Hyeon, *Chem. Soc. Rev.*, 2009, 38, 372.
13. F. Carniato, L. Tei, W. Dastu, L. Marchese and M. Botta, *Chem. Commun.*, 2009, 1246.
14. F. Carniato, C. Bisio, G. Paul, G. Gatti, L. Bertinetti, S. Coluccia and L. Marchese, *J. Mater. Chem.*, 2010, 20(26), 5504.
15. J. Y. Ying, C. P. Mehnert and M. S. Wong, *Angew. Chem., Int. Ed.*, 1999, 38, 56.
16. D. Zhao, Q. Huo, J. Feng, B. F. Chmelka and G. D. Stucky, *J. Am. Chem. Soc.*, 1998, 120, 6024.
17. Y. Wan, Y. Shia and D. Zhao, *Chem. Commun.*, 2007, 897.
18. F. Kleitz, L. A. Solovyov, G. M. Anilkumar, S. H. Choi and R. Ryoo, *Chem. Commun.*, 2004, 1536.
19. Y. K. Hwang, J.-S. Chang, Y.-U. Kwon and S.-E. Park, *Microporous Mesoporous Mater.*, 2004, 68, 21.
20. M. Mesa, L. Sierra, J. Patarin and J.-L. Guth, *Solid State Sci.*, 2005, 7, 990.
21. C. Boissiere, M. Kummel, M. Persin, A. Larbot and E. Prouzet, *Adv. Funct. Mater.* 11 (2001) 129.
22. S.H.B.S. Chan, P.M. Budd, T.D. Naylor, *J. Mater. Chem.* 11 (2001) 951.
23. Y. Sakamoto, M. Kaneda, O. Terasaki, D.Y. Zhao, J.M. Kim, G. Stucky, H.J. Shin, R. Ryoo, *Nature* 408, (2000) 449.
24. P. van der Voort, M. Benjelloun, E.F. Vansant, *J. Phys. Chem. B* 106 (2002) 9027.
25. P. van der Voort, M. Benjelloun, E.F. Vansant, *J. Phys. Chem. B* 106 (2002) 9027.
26. P. Kipkemboi, A. Fogden, V. Alfredsson, K. Flodström, *Langmuir* 17 (2001) 5398.
27. T.W. Kim, R. Ryoo, M. Kruk, K. P. Gierszal, M. Jaroniec, S. Kwon, O. Terasaki, *J. Phys. Chem. B*, 10(2004) 11480.
28. L. Wang, J. Fan, B. Tian, H. Yang, Ch. Yu, B. Tu, D. Zhao, *Microporous Mesoporous Mater.* 67 (2004) 889.
29. C. Yu, J. Fan, B. Tian, D. Zhao, *Chem. Mater.* 16(2004) 889.
30. M. Mesa, L. Sierra, J. Patarin and J.-L. Guth, *Solid State Sci.*, 2005, 7, 990.